Nucleic Acids Research, 2006, Vol. 34, No. 6 ***e46***
doi:10.1093/nar/gkl086

Multiplex degenerate PCR coupled with an oligo sorbent array for human endogenous retrovirus expression profiling

Jean-Philippe Pichon, Bertrand Bonnaud, Philippe Cleuziat[1] and François Mallet*

Unité Mixte de Recherche 2714 CNRS–bioMérieux, IFR128 BioSciences Lyon-Gerland, ENS-Lyon, 46 allée d'Italie, 69364 Lyon cedex 07, France and [1]Centre de Biologie Moléculaire et des Microsystèmes, bioMérieux, Parc Polytec, 5 rue des Berges, 38024 Grenoble Cedex 01, France

Received January 20, 2006; Revised February 7, 2006; Accepted March 7, 2006

ABSTRACT

Human endogenous retroviruses (HERVs) can be divided into distinct families of tens to thousands of paralogous loci. The expression of HERV elements has been detected in all tissues tested to date, particularly germ cells, embryonic tissues and neoplastic tissues. Hence, the study of HERV expression could represent added value in cancer diagnosis. We developed a quantitative assay combining a multiplex degenerate PCR (MD-PCR) amplification, based on the relative conservation of the *pol* genes, and a colorimetric Oligo Sorbent Array (OLISA®). Nine HERV families were selected and amplification primers and capture probes were designed for each family. The features required to achieve efficient amplification of most of the elements of each HERV family and balanced co-amplification of all HERV families were analyzed. We found that MD-PCR reliability, i.e. equivalence of amplification and dose-effect relationship, relied on the adjustment of three critical parameters: the primer degeneracy, the relative concentration of each primer and the total amount of primers in the amplification mixture. The analysis of tumoral versus normal tissues suggests that this assay could prove useful in tumor phenotyping.

INTRODUCTION

Human endogenous retroviruses (HERVs) constitute about 8% of the human genome (1). HERVs are considered as remnants of past germ-cell line infections by retroviruses that occurred during mammal evolution. Phylogenetic studies have identified at least 31 different HERV families each encompassing tens to thousands of loci (2) which are the result of intracellular retrotransposition of transcriptionally active copies. All are defective for viral replication due to genetic drift and are, as a result, transmitted in a Mendelian fashion. Research over the past two decades has demonstrated that HERVs may have biological functions. It has been suggested that HERVs could be involved in genome shaping as potential chromosomal recombination sites (3). HERV long terminal repeats (LTR), whose original function is retroviral expression control, could provide transcriptional regulatory elements for cellular genes consisting in promoter (4), enhancer (5) or polyadenylation signal functions (6). HERV proteins could also have biological functions as illustrated by the ERVWE1 Env protein, also known as syncytin (7–10).

HERV expression was particularly investigated in three specific contexts, i.e. placentation (11,12), auto-immunity (13,14) and cancer (15,16) that are associated with cellular differentiation or immunity modulation. However, it is still generally unclear whether HERVs are triggers or markers in pathological contexts, although it has been suggested that Env HERV-W and Rec HERV-K are involved in multiple sclerosis (17,18) and testicular tumorigenesis (19,20), respectively.

Quantitative approaches concerning both HERV transcripts could thus represent added value in current cancer and chronic disease diagnosis. On the basis of functional hypotheses associated with candidate loci, the majority of HERV quantitative expression studies are based on RT–PCR (11,21–23). Nevertheless, global approaches representing the activity of HERV families may elucidate the mechanisms involved in transcriptional regulation and address physio-pathological functions.

These approaches would consist in analyzing either the expression of each locus within each family or, alternatively, the overall transcription of each family. The first approach is challenging in terms of specificity due to the features of these repeated elements. The second approach could be tackled in two ways, (i) by developing different HERV-taxon specific real-time RT–PCR assays using consensus (24) or degenerate

*To whom correspondence should be addressed. Tel: +33 472 728 358; Fax: +33 472 72 8533; Email: francois.mallet@ens-lyon.fr

primers (25) or (ii) by developing a quantitative assay combining multiplex degenerate PCR (MD-PCR) with an oligonucleotide microarray. This could be achieved subject to minimized bias, i.e. efficient amplification of most of the elements of each family and balanced co-amplification of each family. In this way, the retrovirus *pol* genes reverse-transcriptase region encompasses two conserved sequences, corresponding to the VLPQG and YV/MDDI/V/LL amino-acid motifs, which enabled the development of pan-retrovirus amplifications using degenerate primers. The first pan-retrovirus PCR assay developed by Shih in 1989 (26) was based on a single pair of degenerate primers. This system was improved by adding a semi-nested PCR step (27) which enabled the detection of HERV-W expression in the serum of multiple sclerosis patients (28). Nevertheless, it was established that this system failed to detect the expression of another HERV family (HERV-H) due to a biased degenerate primer composition (29). More sophisticated systems were developed in order to identify all known retroviral reverse-transcriptase sequences. Independent amplifications of beta and gamma retroviruses were obtained initially using two pairs of degenerate primers (30) and at the present time using two complex primer mixtures (31). Interestingly, the report of a broad consistency between the latter qualitative assay and quantitative RT–PCR amplifications (24) suggests that a pan-retrovirus-based procedure could be suitable as a quantitative assay.

In this paper, we describe the development of a pan-retrovirus PCR amplification dedicated to the analysis of differential HERV expression profiles. This aim essentially requires the definition of a quantitative method to evaluate HERV expression. Nine HERV families were selected according to their transcriptional activity in various physio-pathological contexts (HML-2, HML-4, HERV-H, ERV-9, HERV-W, HERV-E4.1 and HERV-R) (32), their sequence homology with infectious retroviruses (HML-5) (33) or their genomic complexity (HERV-L) (34). These families belong to three distinct classes of retroviruses: betaretroviruses (HML-2, HML-4 and HML-5), gammaretroviruses (HERV-H, ERV-9, HERV-W, HERV-E4.1 and HERV-R) and spumaviruses (HERV-L). We systematically investigated the key factors involved in the efficient co-amplification of the nine HERV families. Biotinylated PCR products were quantified using an Oligo Sorbent Array (OLISA®) low-density plastic microarray derived from our Enzyme-linked Oligo Sorbent Assay (ELOSA) developed for the detection and quantitation of HIV1 provirus (35,36). Three parameters were found to be critical in order to obtain an almost equivalent amplification efficiency of the different targets and dose-effect relationship: the primer degeneracy level, the relative concentration of each primer and the total amount of primers in the amplification mixture. Finally, the MD-PCR/OLISA assay was used to compare HERV transcript content in differentiation models and in tumoral versus normal RNA samples.

MATERIALS AND METHODS

Collection of HERV elements

HERV-related sequences were collected from GenBank with RepeatMasker (Smit, AFA, Hubley, R & Green, P. RepeatMasker Open-3.0. 1996–2004 http://www.repeatmasker.org) using a 20% divergence threshold. The query library contained *pol* reference sequences of the nine HERV families, defined as HML-2 (accession no. Y17832, position 4557–7175), HML-4 (AF020092, 3884–6998), HML-5 (AC004536, 36 079–38 642), HERV-H (AJ289709, 2458–6015), ERV-9 (Z84475, 28 749–32 286), HERV-W (AC000064, 32 379–35 878), HERV-E4.1 (M10976, 2650–6210), HERV-R (AC073210, 57 299–60 388), HERV-L (X89211, 2249–5807). Alignments were performed with ClustalW (37) and adjusted manually with the Seaview multiple alignment editors (38). A matrix indicating the occurrence of each nucleotide for each *pol* position was generated in order to design amplification primers and detection probes.

Cloning of HERV-pol archetypes

HERV proviruses were amplified from genomic DNA by means of long-PCR as described previously (10) and *pol* archetypes were then cloned and sequenced after a nested PCR step. Final HERV archetypes were: HML-2 chromosome 7 from base 103 983 434 to 103 984 261, HML-4 chromosome 10 from base 5 074 724 to 5 075 458, HML-5 chromosome 7 from base 117 350 949 to 117 351 816, HERV-H chromosome 2 from base 166 394 420 to 166 395 285, ERV-9 chromosome 6 from base 115 664 573 to 115 665 345, HERV-W chromosome 7 from base 91 746 541 to 91 747 359, HERV-E4.1 chromosome 19 from base 20 726 359 to 20 727 215, HERV-R chromosome 7 from base 63 899 936 to 63 900 787 and HERV-L chromosome 16 from base 59 440 954 to 59 441 771.

Probe design and microarray setup

Fifteen 20–25mer probes corresponding to the nine HERV families were designed within the *pol* amplified region (probe sequences available upon request). For each HERV family, consensus probes were determined using the *pol* sequence matrix. In addition, for the HML-2 capture probe, positions 12, 6, 19, 22 and 3 were cumulatively changed into cytosine to generate from one to five mismatch-containing probes. This type of probe was also designed for HERV-H by mutating the 9th position. The OLISA® microarrays (39) were purchased from bioMérieux (Grenoble, France). They consisted of 8-well plastic modules in which the probes were spotted in a circular format and tethered onto the support by a 5′ aminated end (Figure 1A). Probe specificity was assessed by hybridization with biotinylated transcripts produced from cloned archetypes. HML-2 and HERV-H variant probes were used to evaluate the mismatch impact on target hybridization. The final version of the microarray used to analyze biological samples contained HERV specific validated probes and HIV1- and HTLV1-negative controls.

Primer design

Degenerate primer pairs were designed in a highly conserved region of the *pol* gene RT sub-region. For each of the nine HERV families investigated in the study, the primer sequences were determined according to the corresponding *pol* sequence matrix. The levels of degeneracy were defined in line with the general parsimony principle highlighted in this study. The amplification efficiency and specificity of each degenerate

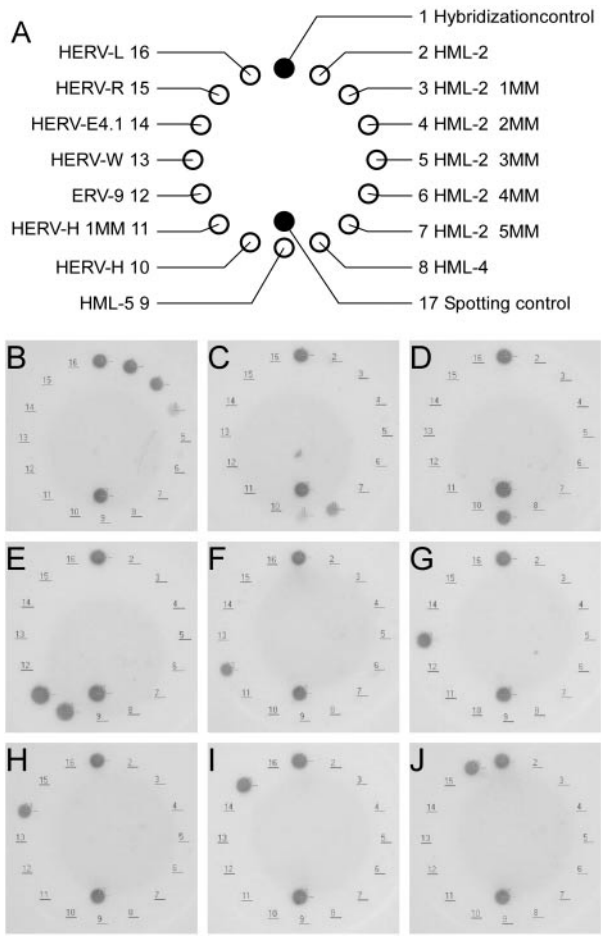

Figure 1. Microarray design. (**A**) Microarray map. The OLISA® microarray comprises a spotting control consisting in a biotinylated oligonucleotide and a hybridization control consisting in an oligonucleotide complementary to the spiked target. HERV-*pol* probe specificity was assessed by hybridization with biotinylated targets: (**B**) HML-2, (**C**) HML-4, (**D**) HML-5, (**E**) HERV-H, (**F**) ERV-9, (**G**) HERV-W, (**H**) HERV-E4.1, (**I**) HERV-R and (**J**) HERV-L.

primer pair was checked on cloned HERV-*pol* archetypes before collecting them to form a global primer mix.

HERV-L-specific amplification

HERV-L PCR amplifications with a weakly-degenerate (Forward tttactgtcctacytcagggr, Reverse tcarcataatgycatcaatgta) or highly-degenerate (Forward ttyactgtcctacctyarrrr, Reverse tcagyataatrycatyartrya) primer pair were carried out in a total volume of 50 µl containing 10 mM Tris–HCl, 1.5 mM $MgCl_2$, 50 mM KCl, 16.5 pmol of each primer, 0.25 mM of each deoxynucleotide triphosphate, 0.25 U of *Taq* polymerase (Roche) and 250 ng of genomic DNA. Amplifications were performed in a GeneAmp® PCR System 9700 thermal cycler (Applied) following modified pan-retrovirus cycling (31): initial 5 min denaturation step at 94°C, 3 cycles at 94°C for 30 s, 45°C for 3 min and 72°C for 1 min followed by 35 cycles at 94°C for 30 s, 50°C for 2 min and 72°C for 1 min, followed by a 7 min final extension step at 72°C. The amplification products were separated by electrophoresis on 3% agarose gel. The bands of interest were purified and cloned in pCR® 2.1-TOPO® vector using the TOPO TA Cloning® Kit (Invitrogen). Twenty two 'weakly-degenerate HERV-L' clones and 24 'highly-degenerate HERV-L' clones were sequenced. A phylogenetic tree was then constructed from these sequences using the UPGMA (absolute distance) method.

Cell culture and differentiation

BeWo b30 human choriocarcinoma cells were cultured in F-12K medium (Invitrogen, Carlsbad, CA) supplemented with 10% fetal calf serum (FCS) (Invitrogen, Carlsbad, USA), antibiotics (100 IU of penicillin/ml and 100 µg of streptomycin/ml) (Invitrogen, Carlsbad, CA) and 0.25 µg/ml amphotericin B (Fungizone) (Invitrogen, Carlsbad, USA). At 50% confluence, the medium was then replaced by one containing 50 µM forskolin (Calbiochem, Darmstadt, Germany) or vehicle (DMSO) (Sigma, St Louis, USA), followed by 36 h of incubation at 37°C to induce BeWo differentiation. U937 monocytoid cells were cultured in RPMI 1640 medium containing 10% FCS, antibiotics (100 IU of penicillin/ml and 100 µg of streptomycin/ml) (Invitrogen, Carlsbad, CA) and 0.25 µg/ml amphotericin B (Fungizone) (Invitrogen, Carlsbad, USA). The cells were seeded at a density of 5.10^5 cells per ml of a culture medium containing 50 ng/ml of phorbol-12-myristate-13-acetate (PMA) or vehicle (DMSO) (Sigma, St Louis, USA), followed by 72 h of incubation at 37°C to induce U937 differentiation. Cultures were performed in triplicate for each set of experiments to assess reproducibility.

RNA samples and reverse-transcription

BeWo b30 and U937 total RNA were isolated using the RNeasy Midi Kit including an on-column DNAse treatment in accordance with the manufacturer's instructions (Qiagen, Hilden, Germany). Breast, colon, lung, prostate, testis and uterus FirstChoice® Human Tumor/Normal Adjacent Tissue RNA was purchased from Ambion (Austin, Texas). The quantity of RNA was measured at OD_{260} in a spectrophotometer and the RNA quality was assessed with a Bioanalyzer capillary electrophoresis device (Agilent, Palo Alto, USA). The total RNA (5 µg or 1 µg from cultured cells or commercial samples, respectively) was reverse transcribed in a volume of 20 µl containing 1× first strand buffer, 0.01 M DTT, 40 U RNaseOUT, 0.5 mM dNTP-Mix, 250 ng of random primers (Promega, Madison, USA) and 200 U of SuperScriptII (Invitrogen, Carlsbad, USA) according to the manufacturer's recommendations. Reverse-transcriptase-free reactions were carried out to verify the absence of contaminating genomic DNA.

Multiplex PCR

Multiplex PCRs were carried out in a total volume of 50 µl containing 10 mM Tris–HCl, 1.5 mM $MgCl_2$, 50 mM KCl, 10 µM (or various concentrations for the optimal concentration range determination) of optimized primer mix, 0.25 mM of dATP, 0.25 mM of dCTP, 0.25 mM of dGTP, 0.188 mM of dTTP, 0.062 mM of dUTP-biotin (Roche), 0.25 U of *Taq* polymerase (Roche) and 5 µl of the reverse-transcription reaction volume or predefined copy number of cloned archetypes. Amplifications were performed in a GeneAmp® PCR System 9700 thermal cycler as follows: initial 5 min denaturation step at 94°C, 3 cycles at 94°C for 30 s, 45°C for 3 min and 72°C for

1 min followed by 20 to 35 cycles at 94°C for 30 s, 50°C for 2 min and 72°C for 1 min, followed by a final 7 min extension step at 72°C. Amplification products were systematically checked by electrophoresis on 3% agarose gel before the microarray analysis.

Microarray analysis

The OLISA® microarray handling and protocol were performed according to the manufacturer's recommendations (bioMérieux, Grenoble, France). In sum: 5 µl of biotin-labeled multiplex amplification products were chemically denatured for 5 min at room temperature (RT), and then hybridized on a microarray for 60 min at 37°C in hybridization solution. The microarrays were washed four times with 300 µl of washing buffer at RT. A detection solution, containing a streptavidine–HRP conjugate, was dispensed on each microarray and incubated for 20 min at 25°C. The microarrays were washed four times with 300 µl of washing buffer at RT. An aliquot of 50 µl of staining solution containing the horseradish peroxidase (HRP) substrate was added to each microarray and incubated for 20 min at 25°C. The microarray image acquisition was then performed using an Apimager® densitometry reader (bioMérieux, Grenoble, France) and the data analysis was performed using the ApiAnalyser software (bioMérieux, Grenoble, France).

Statistical analysis

HERV transcriptome analyses of *in-vitro* differentiation models and tumor/normal adjacent tissue RNA were performed in triplicate. The statistical analysis was performed using Student's *t*-test. The mean values of two groups (mock-treated cells versus treated cells or normal tissue versus tumoral tissue) were considered to be significantly different if $P < 0.05$.

RESULTS

Probe design and validation

The RT moieties of retroviral *pol* genes encompass two highly conserved and closely positioned regions corresponding to the VLPQG and YV/MDDI/V/LL reverse-transcriptase functional motifs. This area was selected to design a multiplex amplification system dedicated to the study of nine HERV families. The alignments of the collected sequences led to the determination of the probability of the presence of the 4 nt on each *pol* consensus position (*pol* sequence matrix). In this way, probes corresponding to the most conserved part of the VLPQG–YV/MDDI/V/LL inner region of each HERV family were designed. Probe specificity was confirmed by the absence of cross-reactions after hybridization with synthetic biotinylated targets (Figure 1B–J). However, the sequence variability existing within each HERV family may result in imperfect complementarities between probes and their homologous targets. Therefore, we evaluated the impact of possible mismatches on target detection using mutation-containing probes. Equivalent signals were measured for HML-2 and HML-2 1MM probes and a weaker but significant signal was measured for HML-2 2MM probes. Similarly, HERV-H and HERV-H 1MM probes displayed comparable signals. Conversely, no signal was detected using HML-2 probes containing more than two mutations.

Degenerate primer design

The primer design was based on the determination of the nucleic acid sequence composition corresponding to the VLPQG and YV/MDDI/V/LL motifs. This constituted a rationale for determining the primer degeneracy. It should be noted that the linear increase of the primer degeneracy level is detrimental to amplification efficiency (sensitivity) due to the geometric increase in combinatory possibilities. The amplification product diversity was used to evaluate the impact of the degeneracy criteria on PCR behavior. The HERV-L family was chosen as a model because it contains the highest number of copies (990) among the nine HERV families and is sufficiently divergent (22%) to discriminate between cloned PCR products. Briefly, PCRs were performed on genomic DNA either with a weakly-degenerate HERV-L-specific primer pair hereafter referred to as Dg4 (level of degeneracy = 4 for each primer) or with a highly-degenerate HERV-L-specific primer pair referred to as Dg128 (level of degeneracy = 128 for each primer) and the PCR products were cloned and sequenced. No bias was obtained using either the Dg128 or the Dg4 primer sets. Firstly, 87.5% (21/24) and 95.5% (21/22) of the sequenced populations consist of distinct clones for Dg128 and Dg4, respectively. Secondly, Dg128 and Dg4 amplification products were found uniformly distributed throughout the phylogenetic tree (Figure 2). In the Dg4 primer set, the lowest frequency observed for a nucleotide position was 83% of that present in the whole HERV-L population alignment. Consequently, for each family, we designed primers by minimizing their level of degeneracy as follows: a single nucleotide or a combination of nucleotides, representing from 100 to 80% of the base frequency observed in the whole population, was determined for each primer position. This led to a mean degeneracy level of 13 ± 16 for the 18 primers. The 80% rule was empirically bypassed in two cases in order to avoid an alteration of the assay sensitivity. For HERV-W, the 78% frequency tolerated for one position of the reverse primer made it possible to halve the primer pair degeneracy. For HERV-E4.1, a 75% frequency tolerated for one position of the forward primer together with a 67% frequency tolerated for one position of the reverse primer made it possible to keep the primer pair degeneracy comparable with other HERV primer pairs (Table 1).

Degenerate primer mix optimization

In a second step, we developed a complex mix of degenerate primers in order to perform a multiplex PCR. The heterogeneity of the level of degeneracy within a primer pair and the heterogeneity of intrinsic amplification efficiencies of primer pairs were taken into account. The primer mix composition was established empirically by PCR amplification of a synthetic model consisting of nine cloned HERV-*pol* archetypes. The amplification performances were compared with a reference equimolar primer mix. An iterative procedure was applied, by constituting several primer mix generations, to define a primer mix resulting in signals as close to each other as possible (Table 1, Figure 3A). The average intensity for the nine HERV families was used as a reference and all

intensities measured were expressed as a percentage of this reference. In this way, the multiplex amplification using the equimolar primer mix resulted in signal intensities widely dispersed around the 100% reference value. The extreme values were 0% for HERV-H and 459% for HML-4. This overall range was dramatically reduced with the final version of the complex primer mix, ranging from 43% for HERV-R to 240% for HML-4. More specifically, six out of nine signals were improved (HML-4, HML-5, HERV-H, HERV-W, HERV-E4.1 and HERV-L), two out of nine signals were unchanged (ERV-9 and HERV-R) and one out of nine was slightly degraded (HML-2: 55% for the equimolar primer mix and 179% for the complex primer mix). Taken together, these results demonstrated that empirical determination of primer quantities in a complex mix compensated for both degeneracy variation in primer pairs and intrinsic amplification efficiency differences. Hence, the complex primer mix developed enabled an equivalent multiplex PCR amplification of nine HERV families. We also studied the impact of the primer concentration on the amplification efficiency of each HERV archetype. We amplified 10^6 copies of each archetype separately with an optimized primer mix concentration range (Figure 3B). The band intensity measurement on the agarose gel electrophoresis pattern led to the determination of an optimal primer mix concentration range in the final reaction volume between 8 and 13 μM. Primer concentrations above 15 μM led to a decrease in the PCR amplification efficiency.

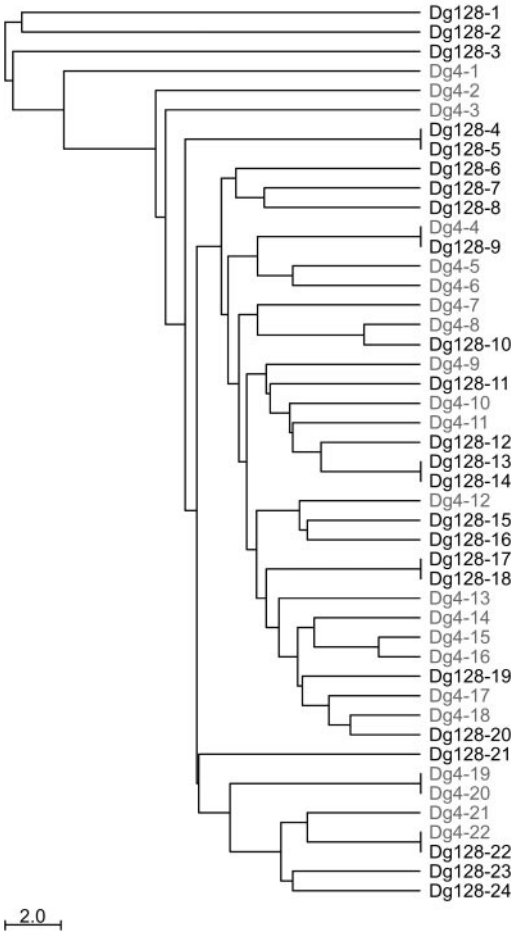

Figure 2. UPGMA (absolute distance) phylogenetic tree of HERV-L amplification products obtained by PCR on genomic DNA. Amplicons generated using weakly-degenerate primers (degeneracy level = 4) are depicted in grey and amplicons generated using strongly-degenerate primers (degeneracy level = 128) are depicted in black.

Multiplex amplification characterization

In order to check whether the defined amplification system co-amplified the nine targets on a 100-fold range of copy numbers efficiently, we performed the amplification of 10-fold serial dilutions of an equimolar mix of archetypes (Figure 4A). These amplifications led to signal variations correlated with target amounts for all HERV archetypes, i.e. with a dose-effect relationship, although with variable dynamic ranges. The broadest dynamic ranges were found for HML-4 (signal intensities from 1773 to 10 320) and HERV-E4.1 (signal intensities from 781 to 9500) and the narrowest was found for HERV-H (signal intensities from 1043 to 1675). However, HML-4 and HERV-H had linear dynamic ranges ($R > 0.99$). Conversely, although it had one of the broadest dynamic ranges, HERV-E4.1 was exponential rather than linear ($R \sim 0.73$). Nevertheless, all these dynamic ranges were found to be compatible with a further quantitation objective. Furthermore, we evaluated the efficiency of the quantitation process for unbalanced target quantities. To this end, four different mixtures of HERV-*pol* archetypes

Table 1. Degenerate primer sequences and primer mix composition

HERV	Forward primer	Dg level[a]	Final concentration (μM)	Reverse primer	Dg level[a]	Final concentration (μM)
HML-2	TRGAAAGTGTTRCCTCARGGA	8	0.51	CACAYAAAATATYATCAAYAYA	16	1.02
HML-4	TGGAAAGTCCTACCACAAGGC	1	0.03	TGCAGAGGAGATCATCCATGTA	1	0.03
HML-5	TRGAAAGTRCTTCCTSAARGR	32	1.02	CYAGTARRATATCATCCATAAA	8	0.51
HERV-H	TGGRCTGTRCTGCYRCAAGGY	32	2.03	AAAGWAGAAGSTCRTCAAWATA	16	1.02
ERV-9	GTCTTGCCHCAAGGGTTT	3	0.13	AGTAAATCATCCACATAYTGAAG	2	0.13
HERV-W	TGGACTGTTTTACCCCAAGGG	1	0.13	AAgTAAATYATCCMYRTACYRA[c]	64	1.02
HERV-E4.1	TGGACCsRGCYTCCCCAARGG[b]	16	1.02	CCAGCARRAGGTCATCaAYSTA[d]	16	1.02
HERV-R	TGGACTAGTCTCCCACAAGGG	1	0.06	CCAAAAGAAGGTTGTCTATGTA	1	0.06
HERV-L	TTTACTGTCCTACYTCAGGGR	4	0.25	TCARCATAATGYCATCAATGTA	4	0.51

[a]Level of degeneracy.
[b]'s' represents 75% of the base(s) observed at that position in the whole population.
[c]'g' represents 78% of the base(s) observed at that position in the whole population.
[d]'a' represents 67% of the base(s) observed at that position in the whole population.

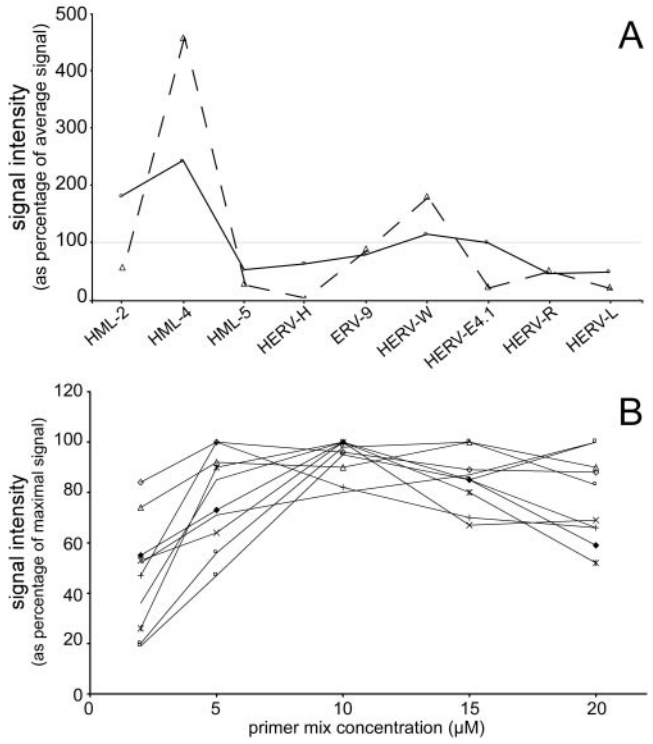

Figure 3. Complex primer mix optimization. (**A**) Equimolar versus complex primer mix amplification product analysis on microarray. A target mix consisting of 10^6 copies of each cloned archetype was amplified either with an equimolar mix of degenerate primers (open triangle and dashed line) or a complex primer mix of degenerate primers (open circle and black line). Band intensities were measured using the Photo-Capt™ software (Vilbert-lourmat, Marne-la-Vallée, France). The average intensity for the nine HERV families was used as a reference and all intensities measured were expressed as a percentage of this reference. (**B**) Optimal complex primer mix concentration range. Each cloned archetype and U937 cDNA were amplified with various final primer mix concentrations (HML-2 large indent, HML-4 open rhombus, HML-5 star, HERV-H open triangle, ERV-9 cross, HERV-W open circle, HERV-E4.1 plus, HERV-R open square, HERV-L small indent and cDNA black rhombus).

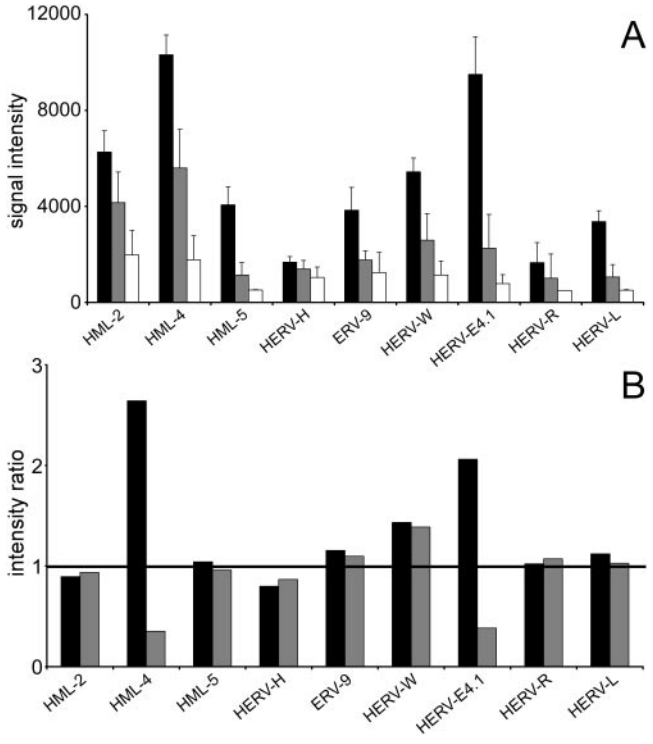

Figure 4. Complex primer mix characterization. (**A**) PCR co-amplification of various target quantities with a complex primer mix. PCRs were performed on target mixtures containing 10^7, 10^6 and 10^5 copies of each HERV archetype, respectively. The mean and standard deviation were calculated from experiments conducted in triplicate. (**B**) Amplification of unbalanced target quantities. Condition A: 10^5 copies of each target, condition B: 10^6 copies of each target, condition C: 10^5 copies of each target, except HML-4 and HERV-E4.1 (10^6 copies) and condition D: 10^6 copies of each target, except HML-4 and HERV-E4.1 (10^5 copies). Black bars represent the C/A ratio of the intensities measured and grey bars represent D/B ratio of the intensities measured. Ratios were calculated from the means of experiments conducted in triplicate. The continuous black line represents a reference value of 1.

were amplified. Mix A and B contained equimolar amounts of each archetype, 10^5 and 10^6 copies, respectively. Mix C contained 10^5 copies of each HERV archetype as for mix A, except for HML-4 and HERV-E4.1 for which the amounts were raised to 10^6 copies. Mix D contained 10^6 copies of each HERV archetype as for Mix B, except for HML-4 and HERV-E4.1 for which the amounts were reduced to 10^5 copies (Figure 4B). The ability of the assay to amplify and to detect the targets independently was evaluated by calculating, for each HERV, the C/A and D/B ratios of the intensities measured. C/A and D/B ratios close to 1 were expected for targets with identical quantities under different experimental conditions. In this way, HML-2, HML-5, HERV-H, ERV-9 HERV-W, HERV-R and HERV-L displayed C/A and D/B ratios ranging from 0.80 to 1.43 and 0.87 to 1.39, respectively. Hence, this demonstrated that the amplification of these seven targets was only affected slightly by the altered amount of the two other targets. Conversely, the increase in the HML-4 and HERV-E4.1 copy numbers under experimental condition C was correlated with a C/A ratio of 2.64 and 2.06, respectively. A reverse alteration of the ratio was observed when the HML-4 and HERV-E4.1 copy numbers were reduced, with the D/B ratio falling to 0.35 and 0.38, respectively. Altogether, these results confirmed the dose-effect relationship previously highlighted and strongly suggested that the amplification system developed could enable the detection of the variation in HERV sequence quantity between different samples.

HERV transcriptome analysis of *in-vitro* differentiation models and tumor/normal adjacent tissue RNAs

MD-PCR/OLISA was used for comparative studies of *in-vitro* cell differentiation models and biological samples. In order to evaluate the reproducibility of the assay, three biological replicates were performed from independent cultures of BeWo, forskolin-induced BeWo, U937 and PMA-stimulated U937 cells. The coefficients of variation (CV = SD/mean) calculated for BeWo cells ranged from 3.3 to 17%, the forskolin-treated BeWo cell CVs ranged from 0.5 to 22.3%, the U937 cell CVs ranged from 3.3 to 24.3% and the PMA-treated U937 cell CVs ranged from 0.5 to 12.2%.

In BeWo cells, forskolin had a significant prominent effect on (i) HML-2, HML-5, and HERV-E4.1 whose expression decreased and on (ii) HERV-W and HERV-R whose expression increased (Figure 5A). In U937 cells, PMA only down-regulated HML-5 and upregulated HERV-R expressions

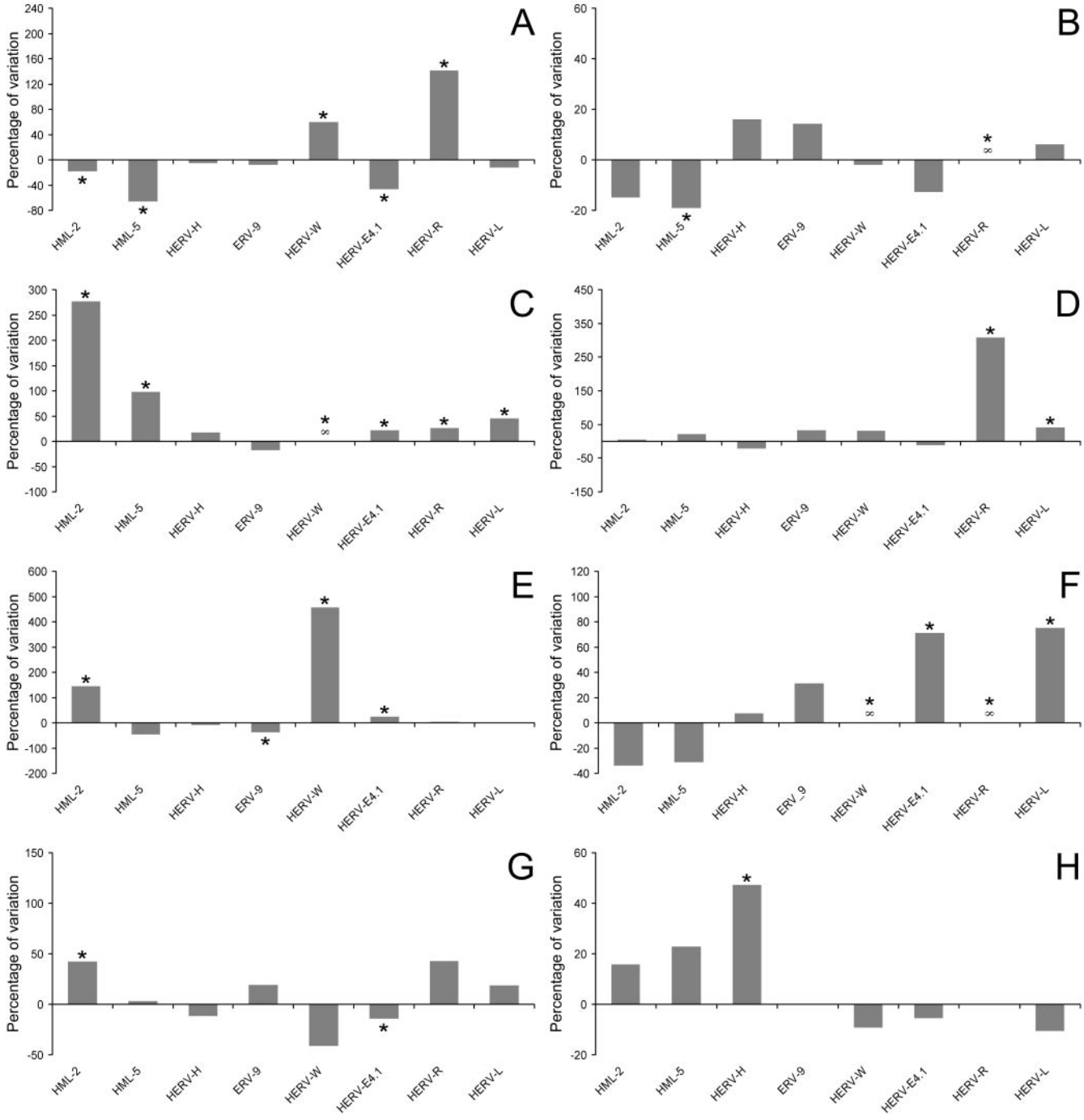

Figure 5. MD-PCR/microarray HERV transcriptome analysis of *in-vitro* differentiation models and paired normal/tumoral RNA. (**A**) Forskolin-treated BeWo b30 cells, (**B**) PMA-treated U937 cells, (**C**) breast, (**D**) uterus, (**E**) testis, (**F**) prostate, (**G**) lung and (**H**) colon. Each bar represents a percentage of signal intensity variation calculated from experiments conducted in triplicate between the differentiated cells or the tumoral tissue and the mock-treated cells or the normal tissue, respectively. The ∞ symbol indicates that a signal was detected for the differentiated cells or the tumoral tissue, whereas no signal was detected for the corresponding mock-treated cells or normal tissue. The Student's *t*-test statistical significance ($P < 0.05$) was indicated by *.

demonstrably (Figure 5B). In this way, inducible modulations of HERV expression in BeWo and U937 cells are specific. Surprisingly, no signal was detected for HML-4 in native or differentiated BeWo and U937 cells. All of the tumor types also demonstrated unique differential expression profiles. The HML-4 family remained untraceable in any of the six sample pairs. Reproductive tissue tumors exhibited unique expression profiles with breast-derived tumor demonstrating statistically significant increases in HML-2, HML-5, HERV-W, HERV-E4.1, HERV-R and HERV-L (Figure 5C), uterine tumor demonstrating HERV-R and HERV-L upregulation (Figure 5D), testicular tumor demonstrating HML-2, HERV-W and HERV-E4.1 upregulation and ERV-9 down-regulation (Figure 5E), and prostate tumor demonstrating

HERV-W, HERV-E4.1, HERV-R and HERV-L upregulation (Figure 5F). Additional tumors, such as those derived from lung and colon also demonstrated unique expression patterns. Lung tumor exhibited an increase in HML-2 transcription and a decrease in HERV-E4.1 expression (Figure 5G) whereas only HERV-H expression increased in colon tumor (Figure 5H). In this way, each cell type or tissue exhibited a unique differential HERV expression profile as opposed to a general increase or decrease in expression.

DISCUSSION

Diagnostic methods have to compromise between specificity and sensitivity, according to the assumed risk of false negative and false positive results, respectively. The biological question addressed in this paper involved two additional problems due to (i) the number of variable loci within each HERV family and (ii) the need for a balanced amplification of all families. Hence, the exhaustiveness and sensitivity of the overall assay are closely linked. This study relates to the identification of general rules allowing the definition of a quantitative assay based on a MD-PCR, coupled with the OLISA® microarray detection format.

In the OLISA® detection format, the exhaustiveness of the capture probe relies upon the empirical selection of the most conserved region, i.e. the consensus, and the experimentally observed ability to tolerate the hybridization of slightly divergent targets as shown using mismatch-containing probes. In this way, the one to two authorized variable sites would make it possible to hybridize not strictly identical loci, e.g. containing polymorphic sites, without generating cross-reactions between different HERV families as depicted. Similarly, no cross-reaction resulted from the use of degenerate amplification primers (see below) as validated using *pol* archetypes. Additionally, a single band of ~130 bp detected by *pol* probes was observed in the agarose gel electrophoresis of MD-PCR products derived from sixteen different RNA samples, strongly suggesting the absence of non-retroviral sequence amplification (data not shown).

In the amplification step, high primer degeneracy should lead to exhaustive but poorly sensitive amplification and, conversely, low primer degeneracy should lead to a poorly exhaustive but sensitive amplification of an HERV family, as highlighted by Forsman *et al*. (25). We defined three critical amplification criteria enabling the quantitation of *pol* gene transcripts of nine HERV families, (i) the primer degeneracy determining exhaustiveness, sensitivity and specificity, (ii) the concentration of each primer determining sensitivity and balanced amplifications and (iii) the total amount of primers in the amplification mixture determining sensitivity. The impact of primer degeneracy on the diversity of the generated amplicons was assessed using the complex HERV-L family. The two experimental populations derived from DNA amplification using either low or high-degenerate HERV-L primers depicted the whole HERV-L population similarly. This enabled us to propose an acceptability threshold to design each primer position, defined as follows: each single nucleotide or combination of nucleotides may represent at least 80% of the base(s) observed at that position in the whole population. In order to minimize the degeneracy level, a lower frequency could be tolerated for a single primer position. In our assay, this concerned 3 out 18 primers and the lowest frequency was 67%.

The degeneracy heterogeneity within each single primer pair may impair the amplification efficiency due to unbalanced availability of reverse versus forward primers toward a given target. This was efficiently counterbalanced by increasing the relative concentration of the more degenerate primer. However, for a primer pair, no linear relationship could be established between the relative degeneracy levels and the optimal primer concentration ratio, as previously mentioned (40). In addition, primer pair concentration was increased for the primer pairs generating weak signals and was decreased for the primer pairs generating strong signals, in order to compensate for their intrinsically heterogeneous amplification efficiencies. This result was found to agree with rules proposed for the development of multiplex PCR (41). The optimal overall primer concentration was found to range between 8 and 13 μM, 10 times higher than in conventional PCR. This MD-PCR primer concentration lies between the 20 μM concentrations described in the original pan-retrovirus degenerate PCR protocol (26) and the 0.5–4 μM concentration range described in various multiplex PCR assays (41–43).

The MD-PCR/OLISA assay detected at least 10^5 copies of each individual archetype in an equimolar mix of all archetypes. This was in the same range as general retroviral PCRs developed by Tuke *et al*. and Seifarth *et al*. (about 1–2.10^6 copies) (25,27,30). This sensitivity is lower than that observed in single-target RT–PCR/ELOSA assays [50 copies, for a review, see (44)], due to primer degeneracy, and lower than that observed in HERV broadly targeted real-time reverse-transcription PCRs (1–10 copies) (25). Nevertheless, this sensitivity is compatible with the detection of moderately expressed genes (10 copies per cell) in view of the nucleic acid quantities used for this assay (~5.10^5 copies in 0.25 μg RNA). A dose-effect relationship was observed within the 10^5–10^7 target range. In addition, a 10-fold difference in target concentrations did not affect the overall amplification efficiency of each distinct target. The robustness of the MD-PCR/OLISA method was assessed on biological replicates consisting of independent RNA extractions, cDNA syntheses, MD-PCR amplifications and OLISA detections. The calculated coefficients of variation ranged from 0.5 to 24.3%. These CVs were found to be comparable to those described using single-target PCR or RT–PCR amplifications coupled with ELOSA monodetection, from 3.0 to 24% (44,45). Hence, the reliability of the MD-PCR/OLISA method is suitable for use as a clinical assay. Moreover, this indicates that the use of both accurate RNA quantitation and quality assessment of RNAs are sufficient to establish total RNA normalization as a suitable method, as previously suggested (46).

We thus investigated the HERV transcriptome modifications occurring in the cell differentiation process and the malignant transformation process. The human choriocarcinoma BeWo cell line undergoes fusion and extensive morphological differentiation, mimicking cytotrophoblast differentiation into syncytiotrophoblasts, following their treatment with cyclic AMP metabolism effectors (47). With the MD-PCR/OLISA assay we confirmed the upregulation of HERV-W and HERV-R in forskolin-treated BeWo Cells (8,48). Similarly, we confirmed HERV-R upregulation in PMA-treated U937 cells (49), an inducible monocyte

differentiation model. However, we did not find significant increases in HERV-W and HERV-H, as previously shown with RT–PCR using *pol* and *gag* primer sets, respectively (21). This may reflect the use of poorly representative *pol* and *gag* primers, inducing increased sensitivity but not reflecting the overall behavior of each family. The MD-PCR/OLISA analysis of normal/tumoral RNA samples led to discriminating profiles between tissues as observed for the two differentiated cell lines. Within these profiles, the observed variations were in agreement with previous independent studies. In this way, the MD-PCR/OLISA assay demonstrated an increase in HML-2 expression in breast tumors (16) and in testicular tumors (50), in HERV-E4.1 expression in prostate tumors (15) and in HERV-H expression in colon tumors (51,52). Surprisingly, no HML-4 expression was detected as opposed to the ubiquitous expression described (24,31), questioning the exhaustiveness/specificity features of both systems. This discrepancy was previously observed in northern blot analyses, showing disparate HML-4 expressions in the lung and placenta (53,54). This illustrates that none of the existing systems are probably exhaustive and that further developments or combinations of assays will be necessary for a comprehensive evaluation of HERV expression. Nevertheless, all profiles were found to be different for the six paired tissues and the two differentiation models. This suggests that the processes involved in the modulation of HERV transcription in the course of (de)differentiation are tissue-specific, as previously suggested (52). Although, it is not known whether identical or different locus subsets of one given HERV family were mobilized, these results demonstrate that the *pol*-based global approach is valid as a profiling tool, as similarly demonstrated for the brain (55). In conclusion, the reliable MD-PCR/OLISA assay we developed provides general rules for the design of multiplex degenerate PCR applications and an alternative system for HERV transcription analysis which may be useful in tumor phenotyping.

ACKNOWLEDGEMENTS

The authors are grateful to C. De Putter for technical assistance and N. Barnes for reading the manuscript. The authors thank anonymous referees for their useful comments. J.Ph.P. was supported by doctoral fellowships from bioMérieux and L'Association Nationale de la Recherche Technique and from L'Association pour la Recherche sur le Cancer. Funding to pay the Open Access publication charges for this article was provided by bioMérieux.

Conflict of interest statement. None declared.

REFERENCES

1. Lander,E.S., Linton,L.M., Birren,B., Nusbaum,C., Zody,M.C., Baldwin,J., Devon,K., Dewar,K., Doyle,M., FitzHugh,W. *et al*. (2001) Initial sequencing and analysis of the human genome. *Nature*, **409**, 860–921.
2. Katzourakis,A. and Tristem,M. (2004) Phylogeny of human endogenous and exogenous retroviruses. In Sverdlov,E. (ed.), *Retroviruses and Primate Genome Evolution*. Landes Bioscience, Georgetown, pp. 1–18.
3. Hughes,J.F. and Coffin,J.M. (2001) Evidence for genomic rearrangements mediated by human endogenous retroviruses during primate evolution. *Nature Genet*., **29**, 487–489.
4. Schulte,A.M., Lai,S., Kurtz,A., Czubayko,F., Riegel,A.T. and Wellstein,A. (1996) Human trophoblast and choriocarcinoma expression of the growth factor pleiotrophin attributable to germ-line insertion of an endogenous retrovirus. *Proc. Natl Acad. Sci. USA*, **93**, 14759–14764.
5. Ruda,V.M., Akopov,S.B., Trubetskoy,D.O., Manuylov,N.L., Vetchinova,A.S., Zavalova,L.L., Nikolaev,L.G. and Sverdlov,E.D. (2004) Tissue specificity of enhancer and promoter activities of a HERV-K(HML-2) LTR. *Virus Res*., **104**, 11–16.
6. Mager,D.L., Hunter,D.G., Schertzer,M. and Freeman,J.D. (1999) Endogenous retroviruses provide the primary polyadenylation signal for two new human genes (HHLA2 and HHLA3). *Genomics*, **59**, 255–263.
7. Blond,J.L., Lavillette,D., Cheynet,V., Bouton,O., Oriol,G., Chapel-Fernandes,S., Mandrand,B., Mallet,F. and Cosset,F.L. (2000) An envelope glycoprotein of the human endogenous retrovirus HERV-W is expressed in the human placenta and fuses cells expressing the type D mammalian retrovirus receptor. *J. Virol*., **74**, 3321–3329.
8. Mi,S., Lee,X., Li,X., Veldman,G.M., Finnerty,H., Racie,L., LaVallie,E., Tang,X.Y., Edouard,P., Howes,S. *et al*. (2000) Syncytin is a captive retroviral envelope protein involved in human placental morphogenesis. *Nature*, **403**, 785–789.
9. Frendo,J.L., Olivier,D., Cheynet,V., Blond,J.L., Bouton,O., Vidaud,M., Rabreau,M., Evain-Brion,D. and Mallet,F. (2003) Direct involvement of HERV-W Env glycoprotein in human trophoblast cell fusion and differentiation. *Mol. Cell Biol*., **23**, 3566–3574.
10. Mallet,F., Bouton,O., Prudhomme,S., Cheynet,V., Oriol,G., Bonnaud,B., Lucotte,G., Duret,L. and Mandrand,B. (2004) The endogenous retroviral locus ERVWE1 is a bona fide gene involved in hominoid placental physiology. *Proc. Natl Acad. Sci. USA*, **101**, 1731–1736.
11. De Parseval,N., Lazar,V., Casella,J.F., Benit,L. and Heidmann,T. (2003) Survey of human genes of retroviral origin: identification and transcriptome of the genes with coding capacity for complete envelope proteins. *J. Virol*., **77**, 10414–10422.
12. Prudhomme,S., Bonnaud,B. and Mallet,F. (2005) Endogenous retroviruses and animal reproduction. *Cytogenet. Genome Res*., **110**, 353–364.
13. Christensen,T., Sorensen,P.D., Hansen,H.J. and Moller-Larsen,A. (2003) Antibodies against a human endogenous retrovirus and the preponderance of env splice variants in multiple sclerosis patients. *Mult. Scler*., **9**, 6–15.
14. Hishikawa,T., Ogasawara,H., Kaneko,H., Shirasawa,T., Matssura,Y., Sekigawa,I., Takasaki,Y., Hashimoto,H., Hirose,S., Handa,S. *et al*. (1997) Detection of antibodies to a recombinant gag protein derived from human endogenous retrovirus clone 4-1 in autoimmune diseases. *Viral Immunol*., **10**, 137–147.
15. Wang-Johanning,F., Frost,A.R., Jian,B., Azerou,R., Lu,D.W., Chen,D.T. and Johanning,G.L. (2003) Detecting the expression of human endogenous retrovirus E envelope transcripts in human prostate adenocarcinoma. *Cancer*, **98**, 187–197.
16. Wang-Johanning,F., Frost,A.R., Jian,B., Epp,L., Lu,D.W. and Johanning,G.L. (2003) Quantitation of HERV-K env gene expression and splicing in human breast cancer. *Oncogene*, **22**, 1528–1535.
17. Antony,J.M., Van Marle,G., Opii,W., Butterfield,D.A., Mallet,F., Yong,V.W., Wallace,J.L., Deacon,R.M., Warren,K. and Power,C. (2004) Human endogenous retrovirus glycoprotein-mediated induction of redox reactants causes oligodendrocyte death and demyelination. *Nature Neurosci*., **7**, 1088–1095.
18. Perron,H., Jouvin-Marche,E., Michel,M., Ounanian-Paraz,A., Camelo,S., Dumon,A., Jolivet-Reynaud,C., Marcel,F., Souillet,Y., Borel,E. *et al*. (2001) Multiple sclerosis retrovirus particles and recombinant envelope trigger an abnormal immune response *in vitro*, by inducing polyclonal Vbeta16 T-lymphocyte activation. *Virology*, **287**, 321–332.
19. Boese,A., Sauter,M., Galli,U., Best,B., Herbst,H., Mayer,J., Kremmer,E., Roemer,K. and Mueller-Lantzsch,N. (2000) Human endogenous retrovirus protein cORF supports cell transformation and associates with the promyelocytic leukemia zinc finger protein. *Oncogene*, **19**, 4328–4336.
20. Boese,A., Galli,U., Geyer,M., Sauter,M. and Mueller-Lantzsch,N. (2001) The Rev/Rex homolog HERV-K cORF multimerizes via a C-terminal domain. *FEBS Lett*., **493**, 117–121.
21. Johnston,J.B., Silva,C., Holden,J., Warren,K.G., Clark,A.W. and Power,C. (2001) Monocyte activation and differentiation augment human endogenous retrovirus expression: implications for inflammatory brain diseases. *Ann. Neurol*., **50**, 434–442.

22. Kudo,Y. and Boyd,C.A. (2002) Changes in expression and function of syncytin and its receptor, amino acid transport system B(0) (ASCT2), in human placental choriocarcinoma BeWo cells during syncytialization. *Placenta*, **23**, 536–541.
23. Buscher,K., Trefzer,U., Hofmann,M., Sterry,W., Kurth,R. and Denner,J. (2005) Expression of human endogenous retrovirus K in melanomas and melanoma cell lines. *Cancer Res.*, **65**, 4172–4180.
24. Seifarth,W., Frank,O., Zeilfelder,U., Spiess,B., Greenwood,A.D., Hehlmann,R. and Leib-Mosch,C. (2005) Comprehensive analysis of human endogenous retrovirus transcriptional activity in human tissues with a retrovirus-specific microarray. *J. Virol.*, **79**, 341–352.
25. Forsman,A., Yun,Z., Hu,L., Uzhameckis,D., Jern,P. and Blomberg,J. (2005) Development of broadly targeted human endogenous gammaretroviral pol-based real time PCRs Quantitation of RNA expression in human tissues. *J. Virol. Methods*, **129**, 16–30.
26. Shih,A., Misra,R. and Rush,M.G. (1989) Detection of multiple, novel reverse transcriptase coding sequences in human nucleic acids: relation to primate retroviruses. *J. Virol.*, **63**, 64–75.
27. Tuke,P.W., Perron,H., Bedin,F., Beseme,F. and Garson,J.A. (1997) Development of a pan-retrovirus detection system for multiple sclerosis studies. *Acta. Neurol. Scand.*, **95**, 16–21.
28. Perron,H., Garson,J.A., Bedin,F., Beseme,F., Paranhos-Baccala,G., Komurian-Pradel,F., Mallet,F., Tuke,P.W., Voisset,C., Blond,J.L. *et al.* (1997) Molecular identification of a novel retrovirus repeatedly isolated from patients with multiple sclerosis. *Proc. Natl Acad. Sci. USA*, **94**, 7583–7588.
29. Christensen,T. (2005) Association of human endogenous retroviruses with multiple sclerosis and possible interactions with herpes viruses. *Rev. Med. Virol.*, **15**, 179–211.
30. Seifarth,W., Krause,U., Hohenadl,C., Baust,C., Hehlmann,R. and Leib-Mösch,C. (2000) Rapid identification of all known retroviral reverse transcriptase sequences with a novel versatile detection assay. *AIDS Res. Hum. Retroviruses*, **16**, 721–729.
31. Seifarth,W., Spiess,B., Zeilfelder,U., Speth,C., Hehlmann,R. and Leib-Mosch,C. (2003) Assessment of retroviral activity using a universal retrovirus chip. *J. Virol. Methods*, **112**, 79–91.
32. Mallet,F. and Prudhomme,S. (2004) [Retroviral inheritance in man]. *J. Soc. Biol.*, **198**, 399–412.
33. Tristem,M. (2000) Identification and characterization of novel human endogenous retrovirus families by phylogenetic screening of the human genome mapping project database. *J. Virol.*, **74**, 3715–3730.
34. Benit,L., Lallemand,J.B., Casella,J.F., Philippe,H. and Heidmann,T. (1999) ERV-L elements: a family of endogenous retrovirus-like elements active throughout the evolution of mammals. *J. Virol.*, **73**, 3301–3308.
35. Mallet,F., Hébrard,C., Brand,D., Chapuis,E., Cros,P., Allibert,P., Besnier,J.M., Barin,F. and Mandrand,B. (1993) Enzyme linked oligosorbent assay for detection of polymerase chain reaction-amplified human immunodeficiency virus type 1. *J. Clin. Microbiol.*, **31**, 1444–1449.
36. Mallet,F., Cros,P. and Mandrand,B. (1995) Enzyme-linked oligosorbent assay for detection of PCR-amplified HIV-1. In Becker,Y. and Darai,G. (eds), *PCR Protocols for Diagnosis of Human and Animal Virus Diseases*. Springer-Verlag, Berlin Heidelberg, pp. 19–28.
37. Thompson,J.D., Higgins,D.G. and Gibson,T.J. (1994) CLUSTAL W: improving the sensitivity of progressive multiple sequence alignment through sequence weighting, position specific gap penalties and weight matrix choice. *Nucleic Acids Res.*, **22**, 4673–4680.
38. Galtier,N., Gouy,M. and Gautier,C. (1996) SEA VIEW and PHYLO_WIN: two graphic tools for sequence alignment and molecular phylogeny. *Comput. Appl. Biosci.*, **12**, 543–548.
39. Perrin,A., Duracher,D., Perret,M., Cleuziat,P. and Mandrand,B. (2003) A combined oligonucleotide and protein microarray for the codetection of nucleic acids and antibodies associated with human immunodeficiency virus, hepatitis B virus, and hepatitis C virus infections. *Anal. Biochem.*, **322**, 148–155.
40. Yang,X. and Marchand,J.E. (2002) Optimal ratio of degenerate primer pairs improves specificity and sensitivity of PCR. *BioTechniques*, **32**, 1002, 1004, 1006.
41. Henegariu,O., Heerema,N.A., Dlouhy,S.R., Vance,G.H. and Vogt,P.H. (1997) Multiplex PCR: critical parameters and step-by-step protocol. *BioTechniques*, **23**, 504–511.
42. Harwood,C.A., Spink,P.J., Surentheran,T., Leigh,I.M., de Villiers,E.M., McGregor,J.M., Proby,C.M. and Breuer,J. (1999) Degenerate and nested PCR: a highly sensitive and specific method for detection of human papillomavirus infection in cutaneous warts. *J. Clin. Microbiol.*, **37**, 3545–3555.
43. Kehl,S.C., Henrickson,K.J., Hua,W. and Fan,J. (2001) Evaluation of the Hexaplex assay for detection of respiratory viruses in children. *J. Clin. Microbiol.*, **39**, 1696–1701.
44. Mallet,F. (2000) Comparison of competitive and positive control-based PCR quantitative procedures coupled with end point detection. *Mol. Biotechnol.*, **14**, 205–214.
45. Mallet,F. (2000) Characterization of RNA using Continuous RT–PCR coupled with ELOSA. In Rapley,R. (ed.), *The Nucleic Acids Protocol Handbook*. Humana Press, Totowa, USA, pp. 219–228.
46. Bustin,S.A. (2002) Quantification of mRNA using real-time reverse transcription PCR (RT–PCR): trends and problems. *J. Mol. Endocrinol.*, **29**, 23–39.
47. Wice,B., Menton,D., Geuze,H. and Schwartz,A.L. (1990) Modulators of cyclic AMP metabolism induce syncytiotrophoblast formation *in vitro*. *Exp. Cell. R.*, **186**, 306–316.
48. Lin,L., Xu,B. and Rote,N.S. (2000) The cellular mechanism by which the human endogenous retrovirus ERV-3 env gene affects proliferation and differentiation in a human placental trophoblast model, BeWo. *Placenta*, **21**, 73–78.
49. Larsson,E., Venables,P.J., Andersson,A.C., Fan,W., Rigby,S., Botling,J., Oberg,F., Cohen,M. and Nilsson,K. (1996) Expression of the endogenous retrovirus ERV3 (HERV-R) during induced monocytic differentiation in the U-937 cell line. *Int. J. Cancer*, **67**, 451–456.
50. Herbst,H., Sauter,M. and Mueller-Lantzsch,N. (1996) Expression of human endogenous retrovirus K elements in germ cell and trophoblastic tumors. *Am. J. Pathol.*, **149**, 1727–1735.
51. Wentzensen,N., Wilz,B., Findeisen,P., Wagner,R., Dippold,W., von Knebel,D.M. and Gebert,J. (2004) Identification of differentially expressed genes in colorectal adenoma compared with normal tissue by suppression subtractive hybridization. *Int. J. Oncol.*, **24**, 987–994.
52. Stauffer,Y., Theiler,G., Sperisen,P., Lebedev,Y. and Jongeneel,C.V. (2004) Digital expression profiles of human endogenous retroviral families in normal and cancerous tissues. *Cancer Immun.*, **4**, 2.
53. Medstrand,P. and Blomberg,J. (1993) Characterization of novel reverse transcriptase encoding human endogenous retroviral sequences similar to type A and type B retroviruses: differential transcription in normal human tissues. *J. Virol.*, **67**, 6778–6787.
54. Seifarth,W., Baust,C., Murr,A., Skladny,H., Krieg-Schneider,F., Blusch,J., Werner,T., Hehlmann,R. and Leib-Mosch,C. (1998) Proviral structure, chromosomal location, and expression of HERV-K-T47D, a novel human endogenous retrovirus derived from T47D particles. *J. Virol.*, **72**, 8384–8391.
55. Frank,O., Giehl,M., Zheng,C., Hehlmann,R., Leib-Mosch,C. and Seifarth,W. (2005) Human endogenous retrovirus expression profiles in samples from brains of patients with schizophrenia and bipolar disorders. *J. Virol.*, **79**, 10890–10901.